



The GlyR Extracellular $\beta 8$ – $\beta 9$ Loop – A Functional Determinant of Agonist Potency

Dieter Janzen^{1†}, Natascha Schaefer^{1†}, Carolyn Delto², Hermann Schindelin² and Carmen Villmann^{1*}

¹ Institute for Clinical Neurobiology, University of Würzburg, Würzburg, Germany, ² Rudolf Virchow Center for Experimental Biomedicine, University of Würzburg, Würzburg, Germany

Ligand-binding of Cys-loop receptors results in rearrangements of extracellular loop structures which are further translated into the tilting of membrane spanning helices, and finally opening of the ion channels. The cryo-EM structure of the homopentameric $\alpha 1$ glycine receptor (GlyR) demonstrated an involvement of the extracellular $\beta 8$ – $\beta 9$ loop in the transition from ligand-bound receptors to the open channel state. Recently, we identified a functional role of the $\beta 8$ – $\beta 9$ loop in a novel startle disease mouse model *shaky*. The mutation of residue GlyR $\alpha 1^{Q177}$ to lysine present in *shaky* mice resulted in reduced glycine potency, reduced synaptic expression, and a disrupted hydrogen network at the structural level around position GlyR $\alpha 1^{Q177}$. Here, we investigated the role of amino acid volume, side chain length, and charge at position Q177 to get deeper insights into the functional role of the $\beta 8$ – $\beta 9$ loop. We used a combined approach of *in vitro* expression analysis, functional electrophysiological recordings, and GlyR modeling to describe the role of Q177 for GlyR ion channel function. GlyR $\alpha 1^{Q177}$ variants do not disturb ion channel transport to the cellular surface of transfected cells, neither in homomeric nor in heteromeric GlyR configurations. The EC₅₀ values were increased for all GlyR $\alpha 1^{Q177}$ variants in comparison to the wild type. The largest decrease in glycine potency was observed for the variant GlyR $\alpha 1^{Q177R}$. Potencies of the partial agonists β -alanine and taurine were also reduced. Our data are further supported by homology modeling. The GlyR $\alpha 1^{Q177R}$ variant does not form hydrogen bonds with the surrounding network of residue Q177 similar to the substitution with a basic lysine present in the mouse mutant *shaky*. Among all investigated Q177 mutants, the neutral exchange of glutamine to asparagine as well as the introduction of the closely related amino acid glutamic acid preserve the hydrogen bond network. Introduction of amino acids with small side chains or larger volume resulted in a loss of their hydrogen bonds to neighboring residues. The $\beta 8$ – $\beta 9$ loop is thus an important structural and functional determinant of the inhibitory GlyR.

Keywords: glycine receptor, $\beta 8$ – $\beta 9$ loop, side chain length, side chain volume, ligand potency, gating, startle disease

Abbreviations: ECD, extracellular domain; GlyR, glycine receptor; TMs, transmembrane domains; WT, wild type.

OPEN ACCESS

Edited by:

Piotr Bregestovski,
Aix-Marseille University, France

Reviewed by:

Alexey Rossokhin,
Research Center of Neurology, Russia
Timothy Lynagh,
University of Copenhagen, Denmark

*Correspondence:

Carmen Villmann
villmann_c@ukw.de

[†]These authors have contributed
equally to this work.

Received: 05 August 2017

Accepted: 22 September 2017

Published: 09 October 2017

Citation:

Janzen D, Schaefer N, Delto C,
Schindelin H and Villmann C (2017)
The GlyR Extracellular $\beta 8$ – $\beta 9$ Loop –
A Functional Determinant of Agonist
Potency.

Front. Mol. Neurosci. 10:322.
doi: 10.3389/fnmol.2017.00322

INTRODUCTION

Glycine receptors (GlyRs) are predominantly expressed in the adult brain stem and spinal cord, where they represent the major component in inhibitory neurotransmission. GlyRs localized in motoneuron membranes in the spinal cord get activated upon glycine release from neighboring inhibitory interneurons. The chloride ion influx leads to hyperpolarization of motoneurons, balancing excitation of the muscle contraction (Rajendra et al., 1997). Disturbances in glycinergic inhibition are associated with rare disorders such as startle disease (OMIM 149400, hyperekplexia, stiff baby syndrome), pain (Harvey et al., 2004), autism spectrum disorders (Harvey and Yee, 2013; Pilorge et al., 2015), and panic disorders (Deckert et al., 2017). Human startle disease is caused by mutations in the *GLRA1*, *GLRB*, and *SLC6A5* genes encoding GlyR subunits $\alpha 1$ and β and the glycine transporter 2 (GlyT2).

Glycine receptors are described as homo- and heteropentameric ligand-gated ion channels of the superfamily of Cys-loop receptors (Lynch, 2004). For heteromeric GlyR complexes, five adjacent subunits are arranged around an ion channel pore composed of two α and three β subunits or three α and two β subunits (Grudzinska et al., 2005; Durisic et al., 2012; Yang et al., 2012). Each GlyR subunit consists of four TM helices, which are connected via intra- or extracellular loop structures. TM2 helices of all five subunits form the inner wall of the ion channel pore. The GlyR ECD is organized into an immunoglobulin-like structure and comprised of a short α -helix and 10 β -strands connected by loop structures (Du et al., 2015; Huang et al., 2015; Moraga-Cid et al., 2015). All Cys-loop receptors share the location of the agonist and antagonist-binding sites in the ECD formed by loops A, B, C from one subunit and loops D, E, F, G from an adjacent subunit (F loop in the following referred to as $\beta 8$ – $\beta 9$ loop) (Brams et al., 2011). Ligands of the GlyR, starting with the highest affinity, are glycine, β -alanine, and taurine (Lynch, 2004). Antagonist of the GlyR is the alkaloid strychnine ($C_{21}H_{22}N_2O_2$) (Breitinger and Becker, 1998). Upon ligand binding, Cys-loop receptors get activated and undergo a variety of conformational changes and transition processes leading to tilts and slight turns of the TM helices and thus opening of the ion pore (Althoff et al., 2014).

Several *in vitro* studies revealed distinct contributions of ECD loop structures for receptor function. It was shown that phenylalanine 159 localized in the loop B contributes to a cation– π interaction with the incoming ligand, which is essential prior to channel opening (Pless et al., 2011). Moreover, loop C plays a role in transmitting the activation signal to the rest of the channel and exhibits a rearrangement upon ligand binding (Althoff et al., 2014). Mutations in the $\beta 2$ – $\beta 3$ loop interfere with the maturation process of the protein and contribute to ligand specificity (Schaefer et al., 2015). Furthermore, loops $\beta 2$ – $\beta 3$ and loop D determine ligand efficacy and play a role in ligand-induced desensitization or channel opening (Nys et al., 2013). The $\beta 8$ – $\beta 9$ loop affects diazepam potentiation of the GABA_ARs (Padgett and Lummis, 2008). Loop $\beta 8$ – $\beta 9$ has been suggested to play a major role in linking ligand binding to channel opening (Khatri and Weiss, 2010). Recently published structural models showed a

coupling of movements within the ECDs, including the $\beta 8$ – $\beta 9$ loop, proceeding to the TM helices resulting in their tilting and enabling ion channel opening and closing (Hassaine et al., 2014; Du et al., 2015; Huang et al., 2015).

We recently published the first *in vivo* model carrying a mutation within the $\beta 8$ – $\beta 9$ loop (Schaefer et al., 2017). A single amino acid exchange GlyR $\alpha 1$ ^{Q177K} in the mouse mutant *shaky* resulted in premature death of homozygous animals. *In vivo*, synaptic GlyRs are decreased generating disturbed glycinergic signal transmission (Schaefer et al., 2017). At the structural level the hydrogen bond network around residue Q177 was disrupted.

Here, we investigated the role of side chain length, volume, and charge at amino acid position 177 in the $\beta 8$ – $\beta 9$ loop of the GlyR $\alpha 1$. Our aim was to understand the importance of $\beta 8$ – $\beta 9$ structural changes with respect to GlyR potency and gating. Our hypothesis is that neutral exchanges and amino acids that preserve the hydrogen network only marginally affect GlyR function. Therefore, we introduced the conservative amino acid exchange GlyR $\alpha 1$ ^{Q177N}. The original mutation in the mouse mutant *shaky* was GlyR $\alpha 1$ ^{Q177K}. We further generated the mutation of glutamine to arginine which is similar to the mutation in *shaky*, but the side chain volume is increased. The series was completed by introduction of small residues, e.g., glycine and alanine, or very large residues such as tryptophan. All residues preserving the hydrogen bond network around residue glutamine 177 had almost no effect on GlyR function. In contrast, residues that were unable to preserve the hydrogen bond network generated functional ion channels with impaired glycine potency. Thus, our data provide further evidence of the GlyR $\beta 8$ – $\beta 9$ loop as a structurally but also functionally important element facilitating inhibitory neurotransmission in the adult organism.

MATERIALS AND METHODS

Site-Directed Mutagenesis

PCR-mutagenesis was used to introduce the mutations (Q177A, Q177C, Q177D, Q177E, Q177G, Q177K, Q177N, Q177R, Q177W) at position 177 (numbering refers to mature protein). The murine GlyR $\alpha 1$ cDNA in the vector pRK7 was used as parental clone and refers to WT. Mutation-carrying amplimers were digested with Pst I and Bam HI and subcloned into the GlyR $\alpha 1$ WT sequence. All mutations were verified by sequencing (LGC Genomics, Berlin, Germany).

Cell Lines

HEK293 human embryonic kidney cells CRL-1573, purchased from ATCC (Manassas, VA, United States) were grown in minimal essential medium (MEM) supplemented with 10% fetal calf serum, 200 mM GlutaMAX, 100 mM sodium pyruvate, and 50 U/ml penicillin/streptomycin (Thermo Fisher Scientific, Waltham, MA, United States) under standard growth conditions at 37°C and 5% CO₂.

Transfection

HEK293 cells were transiently transfected using a modified calcium phosphate precipitation method. A mixture of plasmid

DNA, CaCl_2 , 0.1x TE buffer and 2x HBS (50 mM HEPES, 12 mM glucose, 10 mM KCl, 280 mM NaCl, 1.5 mM Na_2HPO_4) was applied onto the cells. A GlyR α 1 to GlyR β ratio of 1:2 was used for co-expression. For GlyR α 1:GlyR β :GFP co-expression, a ratio of 1:2:1 was transfected. The same amount of DNA was used for GlyR α 1 WT and mutants. Media were exchanged after 6–24 h. Immunocytochemical stainings and electrophysiological experiments were always done 24 h after transfection, biotinylation experiments were performed 48 h after transfection.

Cell Lysates

Whole cell lysates of transfected HEK293 cells transiently expressing the GlyR α 1 variants and GlyR β were acquired by using the CytoBuster Protein Extraction Reagent (Merck Millipore, Billerica, MA, United States) according to the manufacturer's protocol. Forty micrograms of protein were diluted in 2x SDS sample buffer and heated for 5 min at 95°C before use in SDS-PAGE and Western blot.

Biotinylation of Cell Surface Proteins

For biotinylation, transfected HEK293 cells transiently expressing the GlyR α 1 variants or co-expressing GlyR β were used. Medium was aspirated 48 h after transfection and cells were washed once with ice-cold PBS. To label surface proteins, cells were incubated with 1 mg/ml EZ-Link Sulfo-NHS-LC-Biotin (sulfo-succinimidyl-6-[biotin-amido]hexanoate) (Thermo Fisher Scientific, Waltham, MA, United States) for 30 min at 4°C. Cells were washed twice with ice-cold PBS, once with quenching buffer (192 mM glycine, 25 mM TRIS, in PBS pH 8.0) and incubated with quenching buffer for 10 min at 4°C. Cells were scraped into ice-cold PBS, centrifuged for 1 min at 1000 \times g, 4°C, and lysed with 1% Triton X-100, 2 mM EDTA, 0.1 mM PMSE, and 10 mg/ml protease inhibitor (Roche, Basel, Switzerland) in TBS pH 8.0. The lysate was centrifuged again for 1 min at 17000 \times g, 4°C. The supernatant (whole cell fraction, WC) was incubated with 50 μ l of streptavidin agarose beads (Thermo Fisher Scientific, Waltham, MA, United States) using an overhead shaker for 2 h at 4°C. The supernatant (intracellular protein fraction) was removed and beads (surface protein fraction, SF) were washed three times with TBS buffer. The 60 μ l 2x SDS sample buffer was added and the samples were heated 5 min at 95°C before use in SDS-PAGE and Western blot. Before gel loading, the protein amounts of the WC fraction were determined and 40 μ g of protein loaded to each lane of the gel. For SF samples, the same volume (30 μ l) was loaded.

SDS-PAGE and Western Blotting

For protein separation, 11% PAM (polyacrylamide) gels were used. Gels were run at 150 V for 90 min. Proteins were transferred to nitrocellulose (GE Healthcare, Freiburg, Germany) using a wet blot transfer system (transfer buffer: 25 mM TRIS, 192 mM glycine, 10% ethanol) (Bio-Rad, Hercules, CA, United States). For GlyR protein transfer, 2 h at 200 mA were used. For larger proteins, e.g., cadherin, overnight blotting at 100 mA was performed. Membranes were blocked for 1 h with 5% BSA in TBS-T (TBS with 1% Tween 20). Primary antibodies were

incubated overnight at 4°C. Proteins were detected with the pan- α antibody for GlyRs (mAb4a, Synaptic Systems, Göttingen, Germany, Cat. No. 146 011, 1:500) and pan-cadherin (Cell Signaling Technology, Danvers, MA, United States, Cat. No 4068, 1:1500) served as loading control. Signals were detected using the SuperSignal West (Thermo Fisher Scientific, Waltham, MA, United States).

Immunocytochemical Staining

To stain GlyR surface receptors, GlyR α 1 variants, and pDsRed-Monomer-Mem [Takara Bio (formerly Clontech), Mountain View, CA, United States] were co-transfected into HEK293 cells. All steps were performed at room temperature. After fixation for 20 min with 50 μ l 4% paraformaldehyde, 4% sucrose solution, cells were washed three times with PBS and blocked for 30 min with 5% (v/v) goat serum in PBS. Afterward, cells were incubated for 1 h with the GlyR α 1-specific primary antibody mAb2b (1:500 in blocking solution; epitope amino acids 1–10 of mature GlyR α 1; Synaptic Systems, Göttingen, Germany). Cells were washed three times with PBS and incubated for 45 min with the secondary Alexa488-coupled goat-anti-mouse antibody (1:500 in blocking solution; Dianova, Hamburg, Germany). Then, cells were washed three times with PBS, incubated for 5 min with DAPI (1:5000 in PBS; Thermo Fisher Scientific, Waltham, MA, United States) and mounted on glass slides with Mowiol 4-88 (Carl Roth, Karlsruhe, Germany). Imaging was performed using an Olympus IX-81 inverted fluorescence microscope (Olympus, Tokyo, Japan).

Confocal Microscopy, Image Acquisition, and Analysis

Images were acquired using an inverted Olympus IX81 microscope equipped with an Olympus FV1000 confocal laser scanning system, a FVD10 SPD spectral detector and diode lasers of 495 nm (Alexa488) and 550 nm (Cy3) (Olympus, Tokyo, Japan). All images shown were acquired with an Olympus UPLSAPO 60x (oil, numerical aperture: 1.35) objective. The images were further developed and organized by Adobe Photoshop (Adobe, San Jose, CA, United States) or ImageJ (1.51)/Fiji¹.

Electrophysiology

The patch clamp technique was used to measure current amplitudes (I) of transfected HEK293 cells. Currents were amplified using an EPC-9 amplifier and the software Patchmaster (HEKA, Lambrecht, Germany). Cells were patched 24 h after transfection in a whole-cell configuration mode. To measure glycine-evoked chloride currents, 1 mM or 100 μ M glycine were applied. For EC₅₀ measurements, glycine, β -alanine and taurine concentrations ranging from 1–3000 μ M (glycine) or 3–10000 μ M (β -alanine and taurine) were applied. All agonist and antagonists were applied using an Octaflow II system (ALA Scientific Instruments, Farmingdale, NY, United States). The extracellular buffer consisted of (in mM): 137 NaCl, 5.4 KCl, 1.8 CaCl_2 , 1 MgCl_2 , 5 HEPES, pH adjusted to 7.4 with NaOH. The

¹<https://imagej.net/ImageJ>

intracellular buffer contained (in mM): 120 CsCl, 20 N(Et)₄Cl, 1 CaCl₂, 2 MgCl₂, 11 EGTA, 10 HEPES, pH adjusted to 7.2 with CsOH. Recording pipettes with an open resistance of 4–6 M Ω were manufactured from borosilicate capillaries using a P97 horizontal puller (Sutter Instrument, Novato, CA, United States). Cells were held at –60 mV and fast capacitances were in range of 11–13 pF. All experiments were performed at room temperature.

Statistical Analysis

Data analysis of Western blots: The image quantification was performed using ImageJ (1.51)/Fiji². The data were analyzed using Student's *t*-test (analysis of variance) and values below **p* < 0.05 were considered significant, ***p* < 0.01, ****p* < 0.001. The values are displayed as means \pm standard error of the mean (\pm SEM) or as otherwise noted. The graphs were generated using Origin 9.4 software (OriginLab, Northampton, MA, United States).

For the analysis of electrophysiological data, a non-linear algorithm (Origin, OriginLab, Northampton, MA, United States) was used to construct concentration-response curves from peak current amplitudes obtained with eight appropriately spaced concentrations in the range of 1–3000 μ M glycine or 3–10000 μ M β -alanine, and taurine. The following Hill equation was used: $I = I_{max} * c^{n_{Hill}} / (c^{n_{Hill}} + EC_{50}^{n_{Hill}})$. *I* refers to the current amplitude at the given agonist concentration *c*, *I*_{max} is the current amplitude at a saturating agonist, *EC*₅₀ refers to the agonist concentration evoking half-maximal current responses and *n*_{Hill} is the Hill coefficient.

Images were processed with ImageJ (1.51)/Fiji² (Schindelin et al., 2012, 2015; Schneider et al., 2012) and Adobe Photoshop (Adobe, San Jose, CA, United States).

Computational Methods

The effect of different mutations was predicted based on the recent structure of the human homopentameric GlyR $\alpha 3$ in complex with AM-3607 and glycine (Huang et al., 2017). Mutations were introduced *in silico* in the structure and the side chains were positioned in preferred rotamer conformations while minimizing steric overlaps as well as optimizing hydrogen-bonding capabilities using the software Coot (Emsley et al., 2010). Images were made using The PyMOL Molecular Graphics System, Version 1.8 Schrödinger, LLC.

For the alignment the sequences of human GlyR $\alpha 1$, murine GlyR $\alpha 1/\alpha 2/\alpha 3/\beta$, and GABA_A $\alpha 1/\gamma 2$ were aligned with Clustal Omega using the default settings³ (Sievers et al., 2011).

RESULTS

Our current understanding of GlyR ion channel opening and closing suggests concerted movements within the ECD (loops $\beta 9$ – $\beta 10$, $\beta 1$ – $\beta 2$, and $\beta 6$ – $\beta 7$) upon ligand-binding that are transmitted to elements of the ECD-TMD interface ($\beta 10$ -pre-M1,

the M2-3 loop) (Du et al., 2015). The $\beta 8$ – $\beta 9$ loop is part of the ligand-binding site by its localization underneath the ligand-binding pocket (Brejc et al., 2001; Hansen et al., 2005). Recently, we found in a novel startle disease mouse model that a $\beta 8$ – $\beta 9$ loop alteration disrupts GlyR ligand-binding site stability and ion channel gating (Schaefer et al., 2017).

Here, we investigated the role of side chain volume and charge at position Q177 within the $\beta 8$ – $\beta 9$ loop for GlyR expression, agonist potency and structural consequences within the hydrogen bond network of the GlyR ECD.

GlyR $\alpha 1$ Amino Acid Substitutions at Position Glutamine 177 in the $\beta 8$ – $\beta 9$ Loop

Glycine receptors share a large organized N-terminal domain (ECD) with other Cys-loop receptors. The ECD consists of an α -helix, followed by 10 β -strands connected by loop structures important for transmitting conformational changes upon ligand-binding. Residue 177 is localized in the $\beta 8$ – $\beta 9$ loop and occupied by a glutamine in all murine GlyR α subunits, GlyR β as well as human GlyR $\alpha 1$ (Figures 1A,B). The closely related GABA_A receptor subunits $\alpha 1$ and $\gamma 2$ carry a valine ($\alpha 1$) or a glycine ($\gamma 2$) at the corresponding residue in the $\beta 8$ – $\beta 9$ loop (Figure 1B). Mutations within GlyR subunits are associated with human hyperekplexia (Startle disease). The amino acid exchange of Q177 into a lysine resulted in severe startle disease in the mouse mutant *shaky* (Schaefer et al., 2017).

Apart from the GlyR $\alpha 1$ ^{Q177K} mutation in the mouse mutant *shaky*, the following amino acids were introduced at position 177: arginine (GlyR $\alpha 1$ ^{Q177R}) carrying a positively charged side chain similar to lysine in the *shaky* mutant; asparagine (GlyR $\alpha 1$ ^{Q177N}) with a hydrophilic side chain and similar to the original glutamine; aspartate and glutamate (GlyR $\alpha 1$ ^{Q177D}, GlyR $\alpha 1$ ^{Q177E}) both negatively charged; glycine (GlyR $\alpha 1$ ^{Q177G}) a neutral and small amino acid (present in GABA receptor $\gamma 2$); alanine (GlyR $\alpha 1$ ^{Q177A}) with a small hydrophobic side chain; cysteine (GlyR $\alpha 1$ ^{Q177C}) with a thiol side chain; and tryptophan (GlyR $\alpha 1$ ^{Q177W}) carrying a sterically demanding side chain.

$\beta 8$ – $\beta 9$ Loop Alterations with Positive Charged Side Chains at Position Q177 Reduce Surface Expression *In Vitro*

Glycine receptor mutants associated with startle disease affect either GlyR expression or GlyR function. Mutation of GlyR $\alpha 1$ ^{Q177K} resulted in reduced $\alpha 1$ expression *in vitro* [$33 \pm 5\%$ of wild-type $\alpha 1\beta$ (Schaefer et al., 2017)].

Analysis of crude protein lysates (Figures 2A,B) showed protein expression of all GlyR $\alpha 1$ ^{Q177} variants with no overall differences whether co-expressed with GlyR β or when expressed alone. In addition, cell stainings for surface expression also revealed no obvious differences between GlyR $\alpha 1$ WT and GlyR $\alpha 1$ ^{Q177} variants (Figure 2C). GAP-43 expressed as a fusion protein with dsRed encoded on a co-transfected plasmid was used as membrane marker and for control of transfection efficiency. All GlyR $\alpha 1$ ^{Q177} variants exhibited colocalization with GAP-43 and thus cellular surface expression.

²<https://imagej.net/ImageJ>

³<http://www.ebi.ac.uk/Tools/msa/clustalo/>

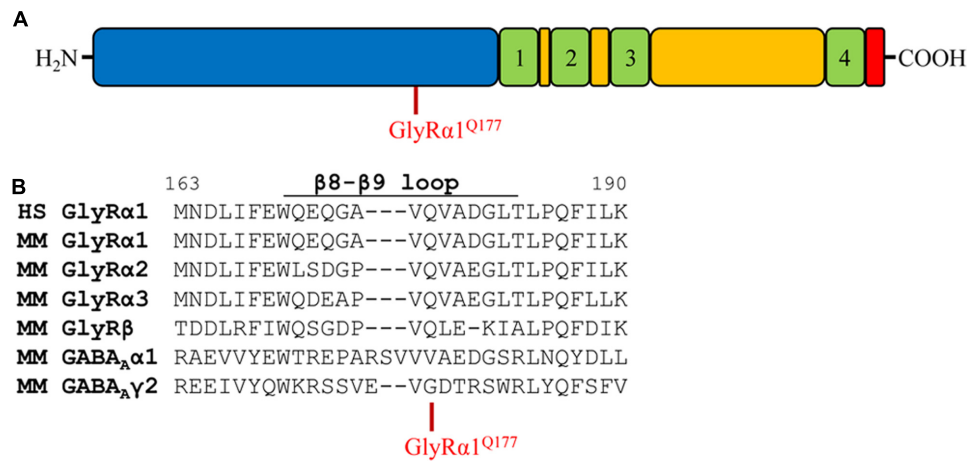


FIGURE 1 | The glycine receptor $\beta 8$ – $\beta 9$ loop. **(A)** Schematic view of the GlyR domain structure containing the N-terminus (blue), transmembrane domains 1–4 (green) connected by loops (yellow), and C-terminus (red). Residue GlyR $\alpha 1^{Q177}$ highlighted in red. **(B)** Sequence alignment of the $\beta 8$ – $\beta 9$ loop and adjacent residues of human (HS) GlyR $\alpha 1$, mouse (MM) GlyR $\alpha 1$, $\alpha 2$, $\alpha 3$, β and mouse GABA_A $\alpha 1$, $\gamma 2$ subunits.

Protein quantification from Western blots after pull-down of biotinylated surface proteins by streptavidin-beads concomitantly demonstrated no significant differences in whole cell (WC) expression for GlyR $\alpha 1^{Q177}$ variants (Figures 3A upper panel, C and Table 1) or GlyR $\alpha 1^{Q177}$ variants coexpressed with GlyR β subunit (Figures 3B upper panel, D and Table 1). The biotinylation method also allows a direct comparison between WC and surface protein fraction (SF) (Figures 3A,B lower panel and Table 1). Note, in the surface fractions of variants GlyR $\alpha 1$ enhanced degradation is visible but also for WT receptors. Only the upper band was used for calculation of the surface protein amount. Degradation might result from maturation deficits, showing that GlyR $\alpha 1^{Q177}$ variants seem to get stuck on their way to the cell surface, most probably in the ER compartment as shown previously for other recessive GlyR $\alpha 1$ variants (Schaefer et al., 2015). However, significant differences of SF protein level were observed for some GlyR $\alpha 1^{Q177}$ variants without or with co-expression with GlyR β (Figures 3C,D). The GlyR expression of the Q177 variants was normalized to expression of pan-cadherin in the same sample serving as a membrane marker control protein. The resulting relative expression of GlyR $\alpha 1$ WT was set to 1 (corresponding to 100%) and the relative expression of the GlyR $\alpha 1$ variants calculated accordingly (Figures 3C,D lower panels and Table 1).

In single expression studies, the SF protein level for GlyR $\alpha 1^{Q177A}$ ($61 \pm 6\%$), GlyR $\alpha 1^{Q177C}$ ($16 \pm 8\%$), GlyR $\alpha 1^{Q177D}$ ($52 \pm 14\%$), GlyR $\alpha 1^{Q177K}$ ($12 \pm 2\%$), GlyR $\alpha 1^{Q177R}$ ($37 \pm 8\%$), and GlyR $\alpha 1^{Q177W}$ ($30 \pm 15\%$) were significantly reduced compared to $\alpha 1$ WT (Figure 3C and Table 1). Variants GlyR $\alpha 1^{Q177E}$, GlyR $\alpha 1^{Q177G}$, GlyR $\alpha 1^{Q177N}$ exhibited surface expression indistinguishable from GlyR $\alpha 1$ WT (Table 1).

In co-expressions with GlyR β , the surface expression levels were lower compared to single expressions. The GlyR complex consists of two α and three β subunits (Grudzinska et al., 2005) which coassemble within the endoplasmic reticulum.

We coexpressed $\alpha 1$ and β in a 1:2 ratio. The low amount of the β subunit during transfection was probably the reason for the lower expression of GlyR $\alpha 1$ variants at the cell surface in $\alpha 1\beta$ co-expressions (Figures 3C,D).

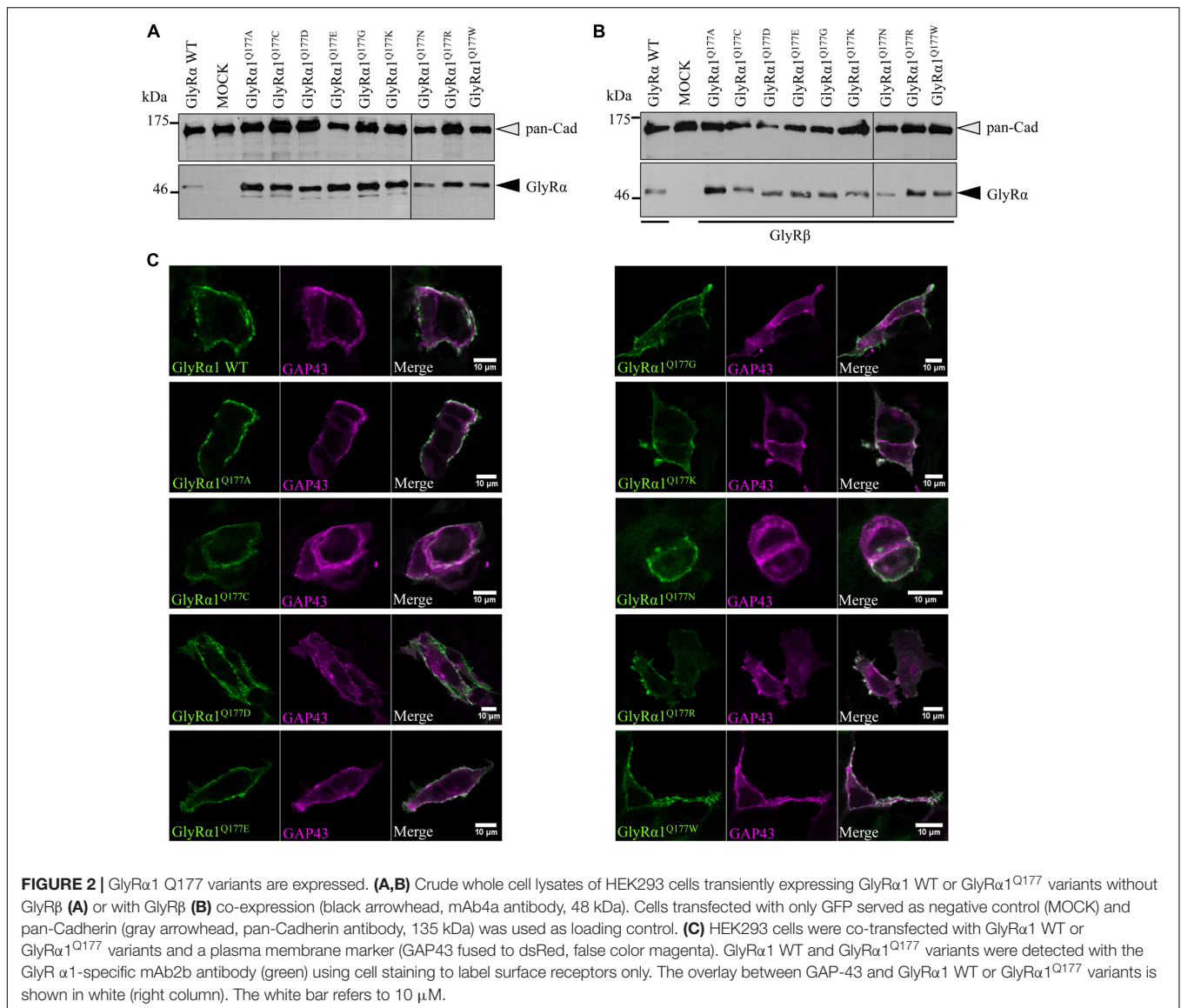
Surface fraction protein level for co-expression with GlyR β demonstrated significant changes: GlyR $\alpha 1^{Q177C}$ ($13 \pm 6\%$), GlyR $\alpha 1^{Q177K}$ ($9 \pm 1\%$), and GlyR $\alpha 1^{Q177W}$ ($13 \pm 3\%$) (Figure 3D and Table 1). Interestingly, the conservative exchange of an asparagine instead of the GlyR $\alpha 1$ WT glutamine had no impact on whole cell and surface expression. The expression of variant GlyR $\alpha 1^{Q177E}$ was also similar to GlyR $\alpha 1$ WT and also did not lead to significant differences in GlyR expression level at the cell surface.

$\beta 8$ – $\beta 9$ Loop Variants Reduce Potency of the Agonist Glycine

Changes in the integrity of the $\beta 8$ – $\beta 9$ loop have been determined to reduce glycine potency and modify the function as a gating element of this receptor class (Schaefer et al., 2017).

Glycine receptor physiology of the mutant receptors coexpressed with the GlyR β subunit was determined by electrophysiological measurements using whole-cell recordings following transient expression in HEK293 cells. As a preliminary screen, absolute currents values (I) were determined at saturating concentrations of glycine (1 mM) and at a glycine concentration around the EC₅₀ value of the GlyR $\alpha 1\beta$ WT (100 μ M). No significant differences in I_{max} values for all GlyR $\alpha 1^{Q177}\beta$ variants in comparison to GlyR $\alpha 1\beta$ WT were observed (Figure 4A) but significant reductions in glycine-induced currents at 100 μ M glycine (Figure 4B and Table 2).

These measurements were followed by a determination of a dose–response curve using eight different glycine concentrations (1, 3, 10, 30, 100, 300, 1000, and 3000 μ M) to determine changes in glycine potency for GlyR $\alpha 1^{Q177}\beta$ variants. An EC₅₀ of 58 ± 4 μ M for GlyR $\alpha 1\beta$ WT was estimated in transfected



HEK293 cells (ratio of 1:2 α 1: β , **Figure 4C**). The glycine EC₅₀ values for GlyR α 1^{Q177} β variants differed in a range between a two-fold (GlyR α 1^{Q177N} β or GlyR α 1^{Q177C} β) up to a six-fold increase (GlyR α 1^{Q177K} β) (**Figures 4C–E** and **Table 2**). Variants were grouped according to structural characteristics. Group one is comprised of GlyR α 1^{Q177K} β and GlyR α 1^{Q177R} β , both positive amino acids which showed a large increase in EC₅₀ when compared to GlyR α 1 β WT (GlyR α 1^{Q177K} β 312 \pm 7 μ M, a 5.3-fold increase and GlyR α 1^{Q177R} β 231 \pm 4 μ M, a 4-fold increase) (**Figure 4C**). The second group consists of the aspartate mutant (negatively charged), the glutamic acid mutant (negatively charged) and the conservative asparagine (polar). The observed increase in EC₅₀, was minor for GlyR α 1^{Q177D} β 137 \pm 4 μ M, a 2.3-fold increase; GlyR α 1^{Q177E} β 109 \pm 7 μ M, a 1.8-fold increase; GlyR α 1^{Q177N} β 96 \pm 1 μ M, a 1.6-fold increase) (**Figure 4D**). The third group includes GlyR α 1^{Q177A} β , GlyR α 1^{Q177C} β , GlyR α 1^{Q177G} β , GlyR α 1^{Q177W} β which all showed

increased EC₅₀ values: GlyR α 1^{Q177A} β 208 \pm 22 μ M, a 3.6-fold increase; GlyR α 1^{Q177G} β 262 \pm 13 μ M, a 4.5-fold increase and GlyR α 1^{Q177W} β 130 \pm 12 μ M, a 2.2-fold increase) (**Figure 4E**). Interestingly, the substituted cysteine with an overall size close to glutamine but rather different to the small residues glycine and alanine or the bulky tryptophan exhibited only a slight shift in glycine potency (88 \pm 3 μ M, a 1.5-fold increase).

To further discriminate between agonist potency and gating defects, we used the GlyR α 1 asparagine mutant (GlyR α 1^{Q177N}), which is closely related to the original glutamine and the arginine mutant (GlyR α 1^{Q177R}) similar to the lysine mutants in the mouse mutant *shaky*. These mutants were analyzed upon application of the partial GlyR agonists β -alanine and taurine.

A concentration of 100 μ M for both partial agonists generated non-significant changes in agonist-induced inward currents with 1.3 \pm 0.3 nA for GlyR α 1 β WT, 0.87 \pm 0.4 nA for GlyR α 1^{Q177N} β ,

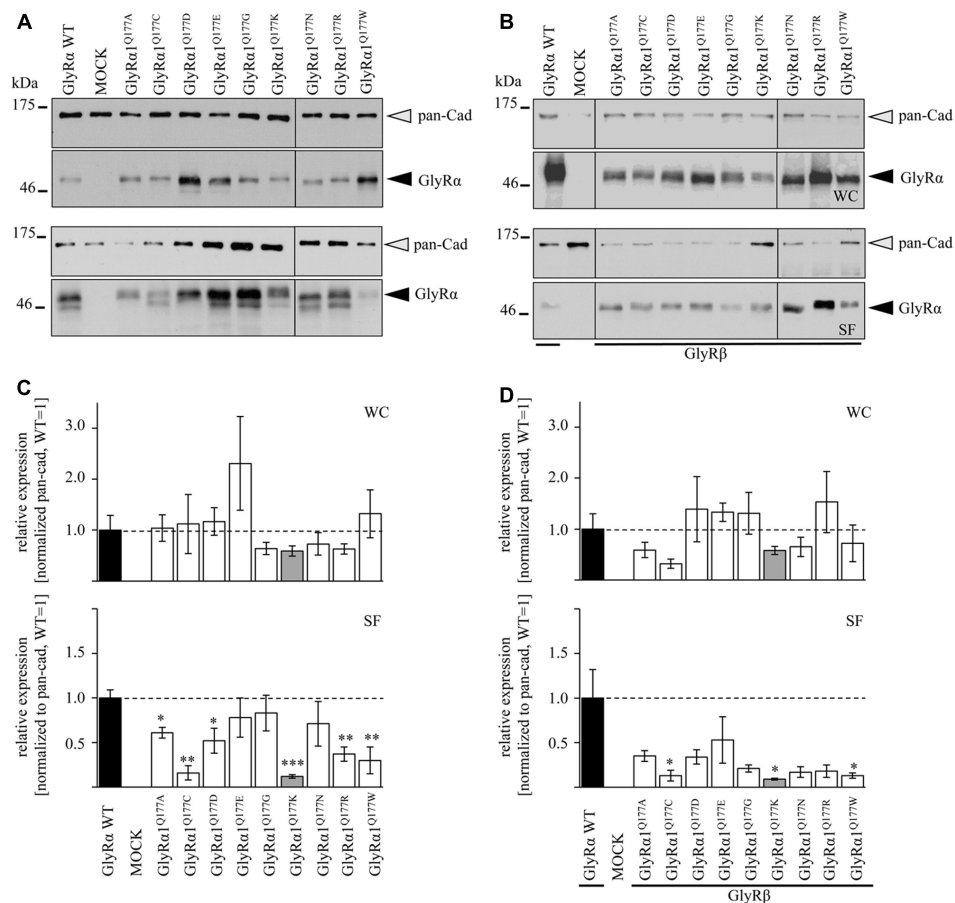


FIGURE 3 | The surface expression is influenced by mutations at position GlyR α 1^{Q177}. **(A,B)** Biotinylation assays were performed to quantify the expression of GlyR α 1^{Q177} variants and distinguish between whole cell (WC) and surface (SF) proteins level. Samples were analyzed by Western blotting using the GlyR pan- α antibody mAb4a (black arrowhead, 48 kDa). Pan-cadherin served as loading control (gray arrowhead, 135 kDa). Cells transfected with only GFP (MOCK) were used as negative control. Three to four independent experiments were performed. Note, an enhanced degradation for variants GlyR α 1^{Q177D}, GlyR α 1^{Q177R}, and GlyR α 1^{Q177W}. Vertical lines indicate that protein bands were taken from different gels of the same experiment. **(C,D)** WC and SF protein levels of independent biotinylation assays without GlyR β **(C)** or with GlyR β **(D)** co-expression were normalized to the loading control pan-cadherin of the same sample and further correlated to GlyR α 1 WT expression which was set to 1 (see dotted line in **(C)** and **(D)**; equals 100%, **Table 1**). Error bars refer to the standard error of the mean (SEM). Level of significance refer to * $p < 0.05$, ** $p < 0.01$, *** $p < 0.001$.

and 0.2 ± 0.07 nA for GlyR α 1^{Q177R} β at 100 μ M β -alanine and 0.13 ± 0.06 nA for GlyR α 1 β WT, 0.02 ± 0.001 nA for GlyR α 1^{Q177N} β , and 0 ± 0 nA for GlyR α 1^{Q177R} β at 100 μ M taurine (**Figures 5A,C**).

The application of 10 mM β -alanine did not result in significant differences between GlyR α 1 β WT (5.3 ± 2 nA, $n = 3$) and GlyR α 1^{Q177N} β (4.1 ± 0.8 nA, $n = 3$) or GlyR α 1^{Q177R} β (4.5 ± 0.9 nA, $n = 3$) (**Figure 5A**). In contrast, taurine application at 10 mM significantly reduced GlyR efficacy with GlyR α 1 β WT 5.7 ± 0.4 nA, $n = 3$; GlyR α 1^{Q177N} β 2.7 ± 0.5 nA, $n = 3$; and GlyR α 1^{Q177R} β 3.1 ± 0.4 nA, $n = 3$ (**Figure 5C**). Although, the GlyR α 1 β WT reached saturation at 10 mM taurine, it is obvious that the mutants probably not completely reached saturation.

Hence, we further examined β -alanine potency in comparison to GlyR α 1 WT, which exhibited a slight increase of the EC₅₀ for β -alanine (GlyR α 1 β WT 157 ± 7 μ M; GlyR α 1^{Q177N} β 203 ± 17 μ M a 1.3-fold increase; GlyR α 1^{Q177R} β 359 ± 19 μ M,

a 2.3-fold increase) (**Figure 5B** and **Table 2**). For taurine potency, the EC₅₀ for the arginine and asparagine GlyR α 1 variants showed the following results in comparison to GlyR α 1 β WT (GlyR α 1 β WT 593 ± 18 μ M; GlyR α 1^{Q177N} β 1254 ± 72 μ M, a 2.1-fold increase; and GlyR α 1^{Q177R} β 2982 ± 183 μ M, a 5-fold increase) (**Figure 5D** and **Table 2**).

In conclusion, the physiological data point to a mixed phenotype affecting agonist/partial agonist potency and most probably partial agonist efficacy at least for taurine.

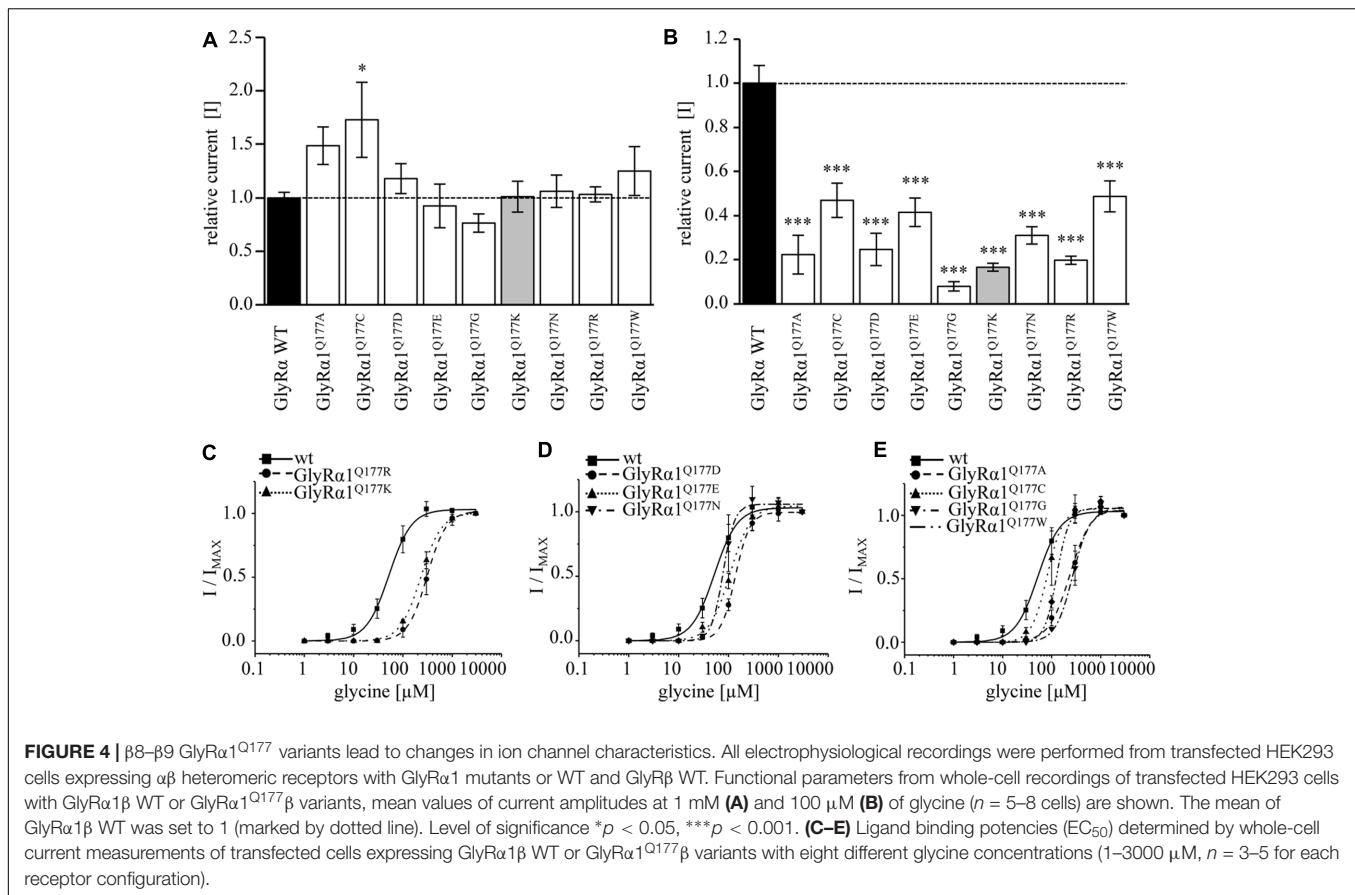
Structural Modeling Revealed Changes in the Hydrogen Bonding Pattern of β 8– β 9 Mutants

Earlier studies reported the importance of the hydrogen bond network within the GlyR ECD or the closely related GABA_A receptor for stabilization of the structure (Padgett and Lummiss,

TABLE 1 | Protein expression profile of GlyR $\alpha 1^{Q177}$ variants.

Construct	Number (n)	Whole cell rel. expression normalized to pan-cad	Significance * <i>p</i> < 0.05, ** <i>p</i> < 0.01, *** <i>p</i> < 0.001	Whole cell rel. expression normalized to pan-cad [%]	Number (n)	Surface rel. expression normalized to pan-cad	Significance * <i>p</i> < 0.05, ** <i>p</i> < 0.01, *** <i>p</i> < 0.001	Surface rel. expression normalized to pan-cad [%]
Single expression								
mAb4a signal (N-domain)								
GlyR $\alpha 1$ WT	4	0.78 ± 0.23		100 ± 30	4	3.02 ± 0.28		100 ± 9
GlyR $\alpha 1^{Q177A}$	4	0.81 ± 0.2	n.s.	102 ± 25	3	1.85 ± 0.19	*	61 ± 6
GlyR $\alpha 1^{Q177C}$	4	0.87 ± 0.45	n.s.	112 ± 58	3	0.47 ± 0.24	**	16 ± 8
GlyR $\alpha 1^{Q177D}$	4	0.91 ± 0.21	n.s.	116 ± 27	4	1.57 ± 0.43	*	52 ± 14
GlyR $\alpha 1^{Q177E}$	4	1.8 ± 0.72	n.s.	230 ± 92	3	2.35 ± 0.65	n.s.	78 ± 22
GlyR $\alpha 1^{Q177G}$	4	0.5 ± 0.09	n.s.	64 ± 12	3	2.51 ± 0.61	n.s.	84 ± 20
GlyR$\alpha 1^{Q177K}$	4	0.46 ± 0.08	n.s.	59 ± 10	3	0.36 ± 0.06	***	12 ± 2
GlyR $\alpha 1^{Q177N}$	4	0.57 ± 0.17	n.s.	73 ± 22	3	2.13 ± 0.76	n.s.	71 ± 25
GlyR $\alpha 1^{Q177R}$	4	0.49 ± 0.08	n.s.	63 ± 10	4	1.12 ± 0.23	**	37 ± 8
GlyR $\alpha 1^{Q177W}$	4	1.03 ± 0.37	n.s.	132 ± 46	3	0.91 ± 0.44	**	30 ± 15
Co-expression with GlyRβ WT								
mAb4a signal (N-domain)								
GlyR $\alpha 1$ WT	5	0.97 ± 0.29		100 ± 30	3	3.36 ± 1.09		100 ± 33
GlyR $\alpha 1^{Q177A}$	4	0.57 ± 0.15	n.s.	59 ± 15	3	1.17 ± 0.19	n.s.	35 ± 6
GlyR $\alpha 1^{Q177C}$	4	0.31 ± 0.09	n.s.	31 ± 9	3	0.44 ± 0.2	*	13 ± 6
GlyR $\alpha 1^{Q177D}$	4	1.35 ± 0.62	n.s.	139 ± 64	3	1.13 ± 0.27	n.s.	33 ± 8
GlyR $\alpha 1^{Q177E}$	4	1.29 ± 0.17	n.s.	133 ± 17	3	1.79 ± 0.88	n.s.	54 ± 27
GlyR $\alpha 1^{Q177G}$	4	1.27 ± 0.4	n.s.	130 ± 41	3	0.71 ± 0.13	n.s.	22 ± 4
GlyR$\alpha 1^{Q177K}$	4	0.56 ± 0.08	n.s.	58 ± 8	3	0.30 ± 0.03	*	9 ± 1
GlyR $\alpha 1^{Q177N}$	4	0.63 ± 0.18	n.s.	65 ± 18	3	0.56 ± 0.21	n.s.	17 ± 6
GlyR $\alpha 1^{Q177R}$	4	1.48 ± 0.58	n.s.	152 ± 60	3	0.59 ± 0.23	n.s.	18 ± 7
GlyR $\alpha 1^{Q177W}$	4	0.7 ± 0.35	n.s.	72 ± 36	3	0.44 ± 0.11	*	13 ± 3

To calculate the relative expression in percent (%), the WT expression was set to 100%. All other estimated relative expression values were calculated accordingly. n.s., non-significant.



2008; Yu et al., 2014). The mutation GlyR α 1^{Q177K} disrupts the hydrogen bond network around residue Q177 (Figures 6A,B). Similarly, the introduction of an arginine at position 177 resulted in lack of hydrogen bonds to neighboring residues such as N42, R65, and N203 (Figure 6C). Interestingly residues that marginally affect GlyR function, such as GlyR α 1^{Q177E} and GlyR α 1^{Q177N} were still able to form a hydrogen bond, arguing for minor structural changes to the GlyR structure (Figures 6D,E). Not in line with a direct correlation between a lack of the hydrogen bond network and large changes in glycine potency are the data on GlyR α 1^{Q177C}. This residue is predicted to lack the hydrogen bonds to R65 and N203 (data not shown), but exhibited only small changes in glycine potency. From its size, cysteine is similar to asparagine. One might therefore argue that size and side chain property underlie the observed effects on glycine potency.

The large side chain volume of GlyR α 1^{Q177W} is expected to completely disrupt the hydrogen bond network (Figure 6F). Similarly, this amino acid exchange resulted in an increased EC₅₀ for the agonist glycine. The correct side chain volume of glutamine at position 177 seems to be critical since tryptophan, the bulkiest side chain, and glycine, the smallest residue, behaved similarly. Glycine most probably is too small and lacks side chain atoms which can engage in the formation of hydrogen bonds, while in the larger residues, the bulkier side chain is no longer able to interact with N42, R65, and N203 (Figure 6F).

DISCUSSION

Signal transduction from ligand-binding into channel opening in Cys-loop receptors involves concerted conformational changes of defined structures of the ECD at both the principle (+) and the complementary (–) site of the intersubunit interface (Hilf and Dutzler, 2008; Hibbs and Gouaux, 2011; Du et al., 2015; Morales-Perez et al., 2016). The involvement of the β 8– β 9 loop in these conformational rearrangements was first described in the cryo-EM structure of the GlyR α 1 subunit analyzing transitions between the closed receptor configuration and the open states (Du et al., 2015).

Previous studies on Cys-loop receptors determined a hydrogen bond network of the β 8– β 9 loop with residues close to the ligand binding site as important for transitions between different receptor states (Padgett and Lummis, 2008; Nys et al., 2013; Yu et al., 2014). Disruptions in structurally important GlyR elements may underlie disease pathology of startle disease (Bode and Lynch, 2014). Several mutations distributed all over the GlyR structure have been correlated to disease mechanisms (Chung et al., 2010).

Within the β 8– β 9 loop one human mutation was so far identified GlyR α 1^{W170S} (Al-Futaisi et al., 2012; Zhou et al., 2013). An RNA-editing variant P185L of the GlyR α 3 β 8– β 9 loop detected in patients with mesial temporal lobe epilepsy (TLE) has been described to increase glycine potency *in vitro* (Meier et al.,

TABLE 2 | Electrophysiological properties of GlyR $\alpha 1^{Q177}$ variants.

$\alpha 1$ construct co-expressed with GlyR β	Number of cells (n)	Mean I_{gly} 100 μM [nA] \pm SEM	Number of cells for EC ₅₀ glycine	EC ₅₀ glycine [μM \pm SEM]	n_H glycine	Number of cells for EC ₅₀ β -alanine	EC ₅₀ β -alanine [μM \pm SEM]	n_H β -alanine	Number of cells for EC ₅₀ taurine	EC ₅₀ taurine [μM \pm SEM]	n_H taurine
GlyR $\alpha 1$ WT	30	3.8 \pm 0.3	5	58 \pm 4	1.9	3	157 \pm 7	2.6	3	593 \pm 18	2.3
GlyR $\alpha 1^{Q177A}$	6	0.8 \pm 0.3***	4	208 \pm 22	2.0		ND			ND	
GlyR $\alpha 1^{Q177C}$	8	1.8 \pm 0.3***	3	88 \pm 3	2.1		ND			ND	
GlyR $\alpha 1^{Q177D}$	6	0.9 \pm 0.3***	5	137 \pm 4	3.4		ND			ND	
GlyR $\alpha 1^{Q177E}$	5	1.6 \pm 0.2***	4	109 \pm 7	2.6		ND			ND	
GlyR $\alpha 1^{Q177G}$	5	0.3 \pm 0.08***	3	262 \pm 13	2.5		ND			ND	
GlyR$\alpha 1^{Q177K}$	5	0.6 \pm 0.07***	3	312 \pm 7	2.2	3	ND	1.7	3	ND	1.6
GlyR $\alpha 1^{Q177N}$	5	1.2 \pm 0.2***	4	96 \pm 1	3.0	3	203 \pm 17		3	1254 \pm 72	
GlyR $\alpha 1^{Q177R}$	5	0.8 \pm 0.07***	4	231 \pm 4	2.0	3	359 \pm 19	1.9	3	2982 \pm 183	1.5
GlyR $\alpha 1^{Q177W}$	5	1.8 \pm 0.3***	3	130 \pm 12	3.7		ND			ND	

Significance values = p ; *** p < 0.001, n , number of cells recorded; n_H hill coefficient; SEM, standard error of the mean; ND, not determined.

2005; Eichler et al., 2009). The murine GlyR $\alpha 1$ startle disease mutant *shaky* (Q177K) resulted in lethality of homozygous animals due to a complex functional pattern including reduced synaptic expression, decreased agonist potency and accelerated ion channel closure (Schaefer et al., 2017). Moreover, glutamine 177 is part of the hydrogen bond network important for ion channel function. Here, we investigated the side chain volume and charge of Q177 with regard to expression and ion channel functionality.

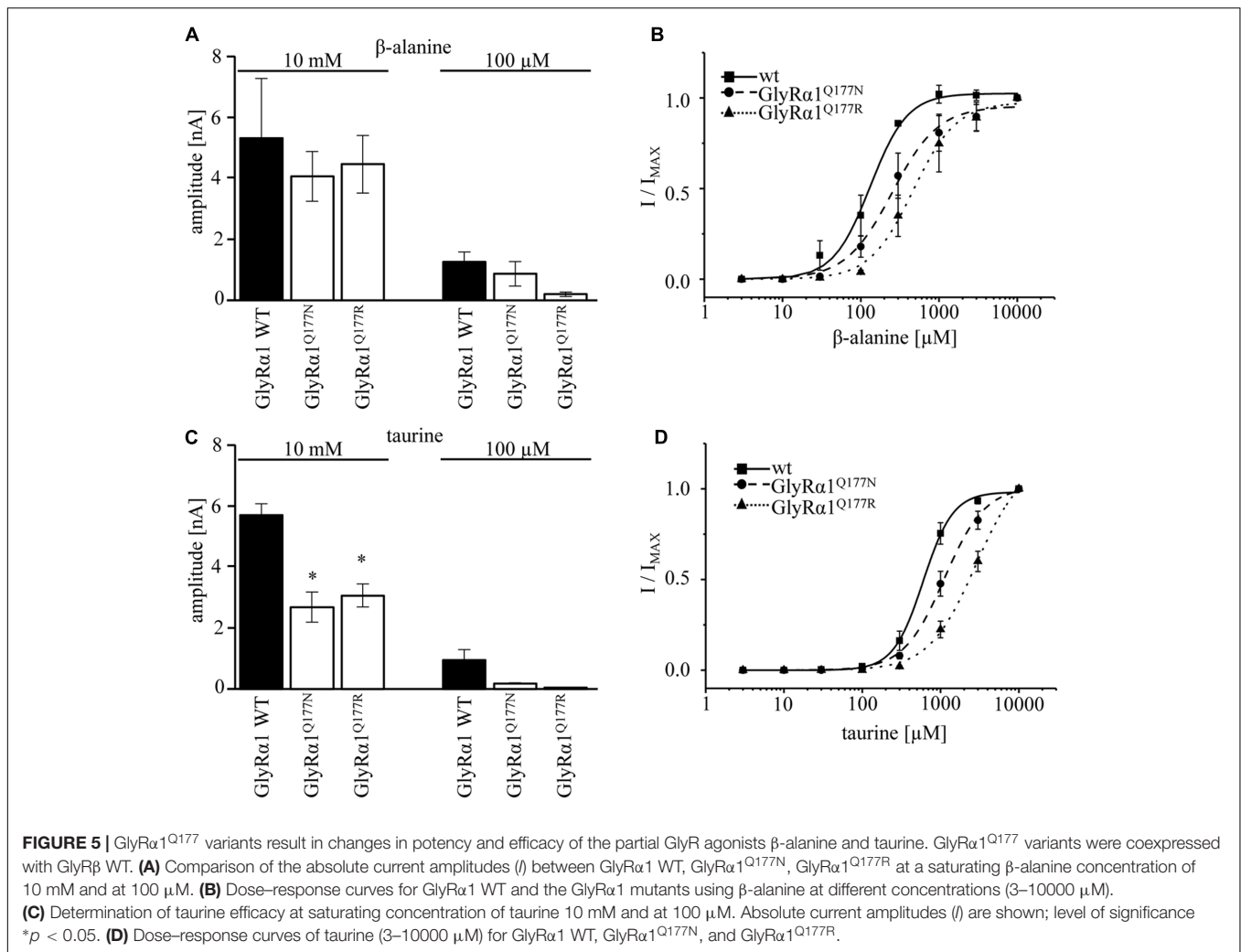
In startle disease, depending on the type of mutation either ion channel function (dominant trait) or expression and transport (recessive mutation) is disabled (Chung et al., 2010; Bode and Lynch, 2014). Although GlyR $\alpha 1^{Q177K}$ leads to decreased expression *in vitro*, there is still enough protein expressed to generate functional ion channels (Schaefer et al., 2017).

For all GlyR $\alpha 1^{Q177}$ variants, the overall expression levels were indistinguishable from $\alpha 1$ WT. Using protein quantification analyses combined with discrimination between whole cell and surface protein, differences between GlyR $\alpha 1$ WT and the mutants were identified. In contrast to no significant differences in the whole cell protein amount of all GlyR $\alpha 1^{Q177}$ variants, surface expression levels differed between WT and mutants.

Similar to the *shaky* variant, GlyR $\alpha 1^{Q177K}$, the mutant GlyR $\alpha 1^{Q177R}$ showed a decreased expression when expressed alone or in co-expression with GlyR β . The conservative exchange of glutamine 177 to asparagine, however, did not result in a different expression pattern in comparison to GlyR $\alpha 1$ WT. Interestingly, the introduction of a negative charge, such as in GlyR $\alpha 1^{Q177E}$ which is a structurally similar amino acid residue to the original glutamine resulted in a similar expression pattern like GlyR $\alpha 1$ WT. The introduction of neutral amino acid residues either small (glycine, alanine, and cysteine) or bulky (tryptophan) resulted in reduced surface receptor levels, independent of the presence of the β -subunit.

A reduction of cell surface receptors argues for differences of maximal currents upon application of saturating glycine concentration. Earlier reports on recessive hyperekplexia mutants demonstrated that a reduction of cellular membrane expression revealed smaller I_{max} values in electrophysiological recordings (Villmann et al., 2009; Chung et al., 2010). The *shaky* mutant GlyR $\alpha 1^{Q177K}$, however, did not result in changes at glycine-induced currents at saturating glycine concentrations although the surface expression was reduced *in vitro* (Schaefer et al., 2017). Here, at a saturating concentration of glycine, all GlyR $\alpha 1^{Q177}$ variants exhibited maximal current amplitudes almost indistinguishable from WT. The estimated reduction of cell surface expression for the GlyR $\alpha 1^{Q177}$ mutants is thus not sufficient to change the maximal current amplitudes in the HEK293 cell overexpression system.

Due to decreased glycinergic currents at lower glycine concentrations observed for all GlyR $\alpha 1^{Q177}$ mutants, a reduction of glycine potency was suggested. Glycine potency was differently affected in GlyR $\alpha 1$ variants. A lower glycine potency was exhibited by GlyR $\alpha 1^{Q177R}$. The determined four-fold decrease of glycine potency was similar to the *shaky* mutation GlyR $\alpha 1^{Q177K}$ (Schaefer et al., 2017). Small changes were observed for the conservative exchange of glutamine to asparagine (1.6-fold) as



well as to the charged glutamate (1.8-fold). The presence of the smallest amino acids glycine and alanine at position 177 revealed higher EC_{50} values for the agonist glycine which were similar to the EC_{50} of the very bulky residue tryptophan.

The $\beta 8$ – $\beta 9$ loop is not directly involved in ligand binding but in structural transitions between agonist bound receptor and the open state of the ion channel (Althoff et al., 2014; Du et al., 2015). No changes in agonist/antagonist affinities have been observed in the *shaky* mouse carrying the GlyR $\alpha 1^{Q177K}$ mutation. Glycine and strychnine bound with the same efficiency to the mutated receptor compared to GlyR $\alpha 1$ WT (Schaefer et al., 2017). The observed glycine potency has been determined to correlate with changes in the hydrogen bond network around residue Q177.

In the variants GlyR $\alpha 1^{Q177K}$ or GlyR $\alpha 1^{Q177R}$ the hydrogen bond with residue R65 is disrupted. In the modeled GlyR $\alpha 1$ WT, the oxygen of the amide at the side chain of glutamine acts as the hydrogen bond acceptor. The side chains of lysine and arginine lack this oxygen, which in turn hinder GlyR $\alpha 1^{Q177K}$ or GlyR $\alpha 1^{Q177R}$ to form a hydrogen bond with R65. Furthermore, the side chains of lysine and arginine are longer compared to glutamine, arguing for steric effects that might be transferred

to conformational changes to the ligand-binding site and thus explain differences in glycine potency.

Asparagine is almost identical in structure to the original glutamine (Q177) in the $\beta 8$ – $\beta 9$ loop with the side chain missing one methylene unit, so one would expect results similar to the GlyR $\alpha 1$ WT. The shorter side-chain of asparagine is predicted to result in a weaker hydrogen bond between GlyR $\alpha 1^{Q177N}$ and R65, as shown in the structural modeling, resulting in a different conformation of the ligand-binding site which probably destabilizes the glycine binding pocket.

While glutamine features an amide, in contrast, glutamic acid carries a carboxyl group. Aspartic acid also features a carboxyl group instead of an amide and misses a methylene unit compared to glutamine. A hydrogen bond between R65 and GlyR $\alpha 1^{Q177D}$ or GlyR $\alpha 1^{Q177E}$ should be possible with an oxygen of the carboxyl group acting as acceptor. However, the negative side chain charge may affect the strength of the hydrogen bond and also the interaction with other nearby structural elements, e.g., N42. Modeling of the putative position of the glutamate side chain showed an orientation toward the amide group of N203, to which it can form tight hydrogen bonds. In contrast, this repositioning

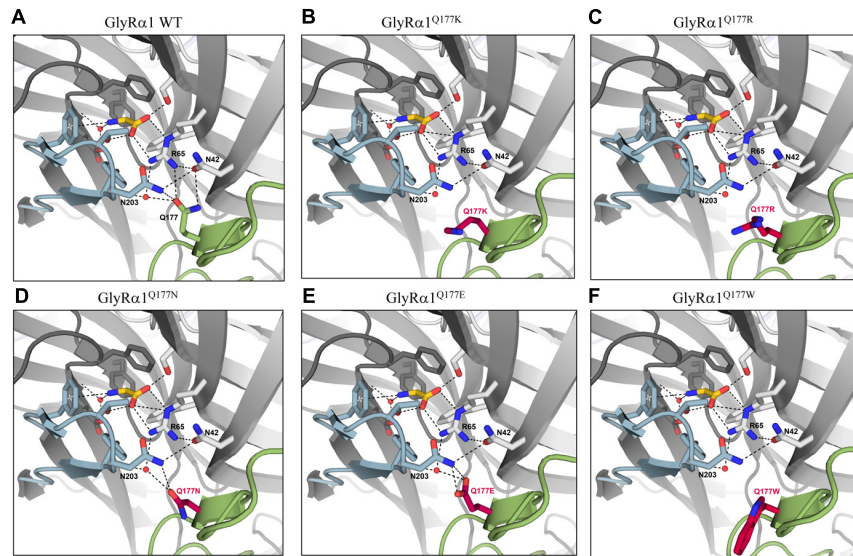


FIGURE 6 | Q177 is localized in a hydrogen bond network important for GlyR function. Q177 is part of a hydrogen-bond network with R65, a critical residue in glycine binding. View into the ligand binding site in the crystal structure of GlyR $\alpha 3$ in complex with AM-3607 and glycine ((Huang et al., 2017) PDB code 5TIN). The principal and complementary subunits are colored gray, respectively. The agonist glycine is shown in yellow, residues that form the ligand binding pocket are marked in blue, Q177 in green or modeled variants **(A)** GlyR $\alpha 1$ WT, **(B)** GlyR $\alpha 1$ ^{Q177K}, **(C)** GlyR $\alpha 1$ ^{Q177R}, **(D)** GlyR $\alpha 1$ ^{Q177N}, **(E)** GlyR $\alpha 1$ ^{Q177E}, and **(F)** GlyR $\alpha 1$ ^{Q177W} at this position in red. Loops C and $\beta 8$ – $\beta 9$ are marked in light blue (loop C) and light green ($\beta 8$ – $\beta 9$). Residues that are engaged in the hydrogen bond network are shown as sticks, relevant water molecules are represented as spheres. Hydrogen bonds (to max. distance of 3.3 Å) are indicated as black dashed lines.

moves the side chain further away from R65 and thereby a second hydrogen bond is lost.

Although, the amino acids glycine and tryptophan differ the most in side chain volume, the determined glycine potency was similarly affected. Glycine has no side chain. Hence, no hydrogen bond between R65 and GlyR $\alpha 1$ ^{Q177G} is possible. Characterization of G160 variants, localized in loop B, revealed that replacing glycine with two other small amino acids alanine and serine results in a 6- to 10-fold decrease in glycine potency (Atak et al., 2015). These data indicate that even the small difference between glycine and alanine can have a big impact on the conformation of the ligand-binding pocket. In contrast, characterization of P250 variants, a residue located in the short intracellular TM1-2 loop, has shown that short side chains gave rise to WT-like channels (Breitinger et al., 2001). Hence, the observed effects depend on the origin of the amino acid at a determined position in the protein.

The introduction of a cysteine at position 177 is also predicted to result in disturbed hydrogen network formation which is in line with a slight rightward shift in glycine EC₅₀ values. Free cysteine residues share the ability for disulfide bridge formation. However, this is unlikely as C138-C152 and C198-C209 already form stable disulfide bridges in the GlyR (James et al., 2013). A disruption of those disulfide bridges would probably have stronger negative effects on ion channel function or even lead to non-functionality (Vogel et al., 2009). Sterically the effect of GlyR $\alpha 1$ ^{Q177C} is less detrimental which might explain the observed small effects on glycine potency. Tryptophan (W) is the largest amino acid and contains an aromatic indole ring. Because of the indole side chain, no hydrogen bond between

GlyR $\alpha 1$ ^{Q177W} and R65 is possible. The original glutamine 177 forms a hydrogen bond with R65, which is located in the glycine binding pocket. Mutation of R65 to lysine and alanine revealed a 200- and 1250-fold decrease in glycine EC₅₀, demonstrating that R65 is an important residue for ligand binding (Grudzinska et al., 2005).

The analysis of partial agonist efficacy and potency implies changes in agonist efficacy at least for taurine and changes in partial agonist potencies. These data indicate that Q177 influences the formation of the agonist/partial agonist binding sites possibly by differences in hydrogen bond network formation. Moreover, taurine measurements verified that structural changes in the $\beta 8$ – $\beta 9$ loop also affect GlyR gating similar to findings for the *shaky* mouse mutant (Schaefer et al., 2017). In summary, the number of contacts to the hydrogen bond network and a mutual stabilization of the conformation seems to be reduced.

Since, the first description of the large movements the $\beta 8$ – $\beta 9$ loop undergoes upon transition from the agonist-bound GlyR structure to the open conformation in the cryo-EM structure of GlyR $\alpha 1$ (Du et al., 2015), similar observations have been explored in the $\alpha 4\beta 2$ crystal structure of the nicotinic acetylcholine receptor (Morales-Perez et al., 2016). The $\beta 8$ – $\beta 9$ loop is connected to loop C covering the binding pocket but also is located underneath the binding pocket, thus it indirectly participates in the binding pocket. Furthermore, it is involved in the coupling of conformational changes of the ECD following ligand binding to finally ion channel opening and closing. During GlyR ion channel opening, the C loop switches from open to closed and displaces the $\beta 8$ – $\beta 9$ loop which concomitantly induces

rotation of the pre-M1 and M1 and finally movement of the M2 elements (Du et al., 2015). The analysis of the first mouse mutant carrying an amino acid transition in the $\beta 8$ – $\beta 9$ loop further revealed the importance of this loop structure for GlyR function and survival. The mutant mouse showed no changes in agonist affinity but the ensuing signal transduction resulting in ion channel opening was almost completely abolished (Schaefer et al., 2017). We showed that all mutations at residue Q177 lack the potential to form hydrogen bonds with residue R65. Thus, the hydrogen bond to R65 is critical for the stabilization of the glycine-binding pocket, which is in agreement with the observed decrease in glycine potencies. A further impact on GlyR gating as suggested by the observed reduced efficacy of the partial agonist taurine is in line with the displacement $\beta 8$ – $\beta 9$ undergoes during GlyR ion channel opening and closing and glycinergic signaling toward the pore forming unit (Du et al., 2015).

Moreover, the $\beta 8$ – $\beta 9$ loop harbors a structural potential for allosteric modulation. Nys et al. (2016) argued that chlorpromazine bound to ELLC, a member of the Cys-loop receptor family, undergoes hydrophobic interaction with $\beta 8$ – $\beta 9$ loop residues and is part of a multisite model for allosteric modulation in a continuous stretch from the top to the bottom of the receptor. A modulatory role of the $\beta 8$ – $\beta 9$ loop has also been determined for GABA_A receptors. Tricyclic oxazole-2,3-benzodiazepines bind to the interface between α and β subunits to residues ¹⁷²REPAR¹⁷⁶ within the GABA_A receptor $\beta 8$ – $\beta 9$ loop. These residues undergo interactions with residues R66 and F45 located close to the agonist binding site (Mihalik et al., 2017). The $\beta 8$ – $\beta 9$ of the GlyR and other Cys-loop

receptors might also harbor allosteric potential for yet unknown modulators.

CONCLUSION

The $\beta 8$ – $\beta 9$ loop is an important contributor to the hydrogen bond network in the ligand-bound state thus stabilizing the glycine-binding pocket.

AUTHOR CONTRIBUTIONS

CV participated in research design. CV and DJ conducted experiments. CD, HS, CV, NS, and DJ performed data analysis. CV and NS wrote the manuscript.

FUNDING

This work was supported by DFG VI586 (CV) and Schi425/8-1 (HS), NS is supported by the SCIENTIA program University Würzburg and DJ is supported by the GLS Würzburg.

ACKNOWLEDGMENT

Gudrun Schell and Nadine Vornberger are highly acknowledged for their excellent technical assistance.

REFERENCES

- Al-Futaisi, A. M., Al-Kindi, M. N., Al-Mawali, A. M., Koul, R. L., Al-Adawi, S., and Al-Yahyaee, S. A. (2012). Novel mutation of *GLRA1* in Omani families with hyperekplexia and mild mental retardation. *Pediatr. Neurol.* 46, 89–93. doi: 10.1016/j.pediatrneurol.2011.11.008
- Althoff, T., Hibbs, R. E., Banerjee, S., and Gouaux, E. (2014). X-ray structures of GluCl in apo states reveal a gating mechanism of Cys-loop receptors. *Nature* 512, 333–337. doi: 10.1038/nature13669
- Atak, S., Langhofer, G., Schaefer, N., Kessler, D., Meiselbach, H., Delto, C., et al. (2015). Disturbances of ligand potency and enhanced degradation of the human glycine receptor at affected positions G160 and T162 originally identified in patients suffering from hyperekplexia. *Front. Mol. Neurosci.* 8:79. doi: 10.3389/fnmol.2015.00079
- Bode, A., and Lynch, J. W. (2014). The impact of human hyperekplexia mutations on glycine receptor structure and function. *Mol. Brain* 7:2. doi: 10.1186/1756-6606-7-2
- Brams, M., Pandya, A., Kuzmin, D., van Elk, R., Krijnen, L., Yakel, J. L., et al. (2011). A structural and mutagenic blueprint for molecular recognition of strychnine and d-tubocurarine by different cys-loop receptors. *PLoS Biol.* 9:e1001034. doi: 10.1371/journal.pbio.1001034
- Breitinger, H. G., and Becker, C. M. (1998). The inhibitory glycine receptor: prospects for a therapeutic orphan? *Curr. Pharm. Des.* 4, 315–334.
- Breitinger, H. G., Villmann, C., Becker, K., and Becker, C. M. (2001). Opposing effects of molecular volume and charge at the hyperekplexia site alpha 1(P250) govern glycine receptor activation and desensitization. *J. Biol. Chem.* 276, 29657–29663. doi: 10.1074/jbc.M100446200
- Brejč, K., van Dijk, W. J., Klaassen, R. V., Schuurmans, M., van Der Oost, J., Smit, A. B., et al. (2001). Crystal structure of an ACh-binding protein reveals the ligand-binding domain of nicotinic receptors. *Nature* 411, 269–276. doi: 10.1038/35077011
- Chung, S. K., Vanbellinthen, J. F., Mullins, J. G., Robinson, A., Hantke, J., Hammond, C. L., et al. (2010). Pathophysiological mechanisms of dominant and recessive *GLRA1* mutations in hyperekplexia. *J. Neurosci.* 30, 9612–9620. doi: 10.1523/JNEUROSCI.1763-10.2010
- Deckert, J., Weber, H., Villmann, C., Lonsdorf, T. B., Richter, J., Andreatta, M., et al. (2017). *GLRB* allelic variation associated with agoraphobic cognitions, increased startle response and fear network activation: a potential neurogenetic pathway to panic disorder. *Mol. Psychiatry* 22, 1431–1439. doi: 10.1038/mp.2017.2
- Du, J., Lu, W., Wu, S., Cheng, Y., and Gouaux, E. (2015). Glycine receptor mechanism elucidated by electron cryo-microscopy. *Nature* 526, 224–229. doi: 10.1038/nature14853
- Duricic, N., Godin, A. G., Wever, C. M., Heyes, C. D., Lakadamyali, M., and Dent, J. A. (2012). Stoichiometry of the human glycine receptor revealed by direct subunit counting. *J. Neurosci.* 32, 12915–12920. doi: 10.1523/JNEUROSCI.2050-12.2012
- Eichler, S. A., Förstera, B., Smolinsky, B., Jüttner, R., Lehmann, T. N., Fähling, M., et al. (2009). Splice-specific roles of glycine receptor $\alpha 3$ in the hippocampus. *Eur. J. Neurosci.* 30, 1077–1091. doi: 10.1111/j.1460-9568.2009.06903.x
- Emsley, P., Lohkamp, B., Scott, W. G., and Cowtan, K. (2010). Features and development of Coot. *Acta Crystallogr. D Biol. Crystallogr.* 66, 486–501. doi: 10.1107/S0907444910007493
- Grudzinska, J., Schemm, R., Haeger, S., Nicke, A., Schmalzing, G., Betz, H., et al. (2005). The beta subunit determines the ligand binding properties of synaptic glycine receptors. *Neuron* 45, 727–739. doi: 10.1016/j.neuron.2005.01.028
- Hansen, S. B., Sulzenbacher, G., Huxford, T., Marchot, P., Taylor, P., and Bourne, Y. (2005). Structures of Aplysia AChBP complexes with nicotinic agonists and antagonists reveal distinctive binding interfaces and conformations. *EMBO J.* 24, 3635–3646. doi: 10.1038/sj.emboj.7600828
- Harvey, R. J., Depner, U. B., Wassle, H., Ahmadi, S., Heindl, C., Reinold, H., et al. (2004). GlyR $\alpha 3$: an essential target for spinal PGE2-mediated

- inflammatory pain sensitization. *Science* 304, 884–887. doi: 10.1126/science.1094925
- Harvey, R. J., and Yee, B. K. (2013). Glycine transporters as novel therapeutic targets in schizophrenia, alcohol dependence and pain. *Nat. Rev. Drug Discov.* 12, 866–885. doi: 10.1038/nrd3893
- Hassaine, G., Deluz, C., Grasso, L., Wyss, R., Tol, M. B., Hovius, R., et al. (2014). X-ray structure of the mouse serotonin 5-HT₃ receptor. *Nature* 512, 276–281. doi: 10.1038/nature13552
- Hibbs, R. E., and Gouaux, E. (2011). Principles of activation and permeation in an anion-selective Cys-loop receptor. *Nature* 474, 54–60. doi: 10.1038/nature10139
- Hilf, R. J., and Dutzler, R. (2008). X-ray structure of a prokaryotic pentameric ligand-gated ion channel. *Nature* 452, 375–379. doi: 10.1038/nature06717
- Huang, X., Chen, H., Michelsen, K., Schneider, S., and Shaffer, P. L. (2015). Crystal structure of human glycine receptor-alpha3 bound to antagonist strychnine. *Nature* 526, 277–280. doi: 10.1038/nature14972
- Huang, X., Shaffer, P. L., Ayube, S., Bregman, H., Chen, H., Lehto, S. G., et al. (2017). Crystal structures of human glycine receptor alpha3 bound to a novel class of analgesic potentiators. *Nat. Struct. Mol. Biol.* 24, 108–113. doi: 10.1038/nmsb.3329
- James, V. M., Bode, A., Chung, S. K., Gill, J. L., Nielsen, M., Cowan, F. M., et al. (2013). Novel missense mutations in the glycine receptor beta subunit gene (GLRB) in startle disease. *Neurobiol. Dis.* 52, 137–149. doi: 10.1016/j.nbd.2012.12.001
- Khatri, A., and Weiss, D. S. (2010). The role of Loop F in the activation of the GABA receptor. *J. Physiol.* 588, 59–66. doi: 10.1113/jphysiol.2009.179705
- Lynch, J. W. (2004). Molecular structure and function of the glycine receptor chloride channel. *Physiol. Rev.* 84, 1051–1095. doi: 10.1152/physrev.00042.2003
- Meier, J. C., Henneberger, C., Melnick, I., Racca, C., Harvey, R. J., Heinemann, U., et al. (2005). RNA editing produces glycine receptor $\alpha 3^{P185L}$, resulting in high agonist potency. *Nat. Neurosci.* 8, 736–744. doi: 10.1038/nn1467
- Mihalik, B., Palvolgyi, A., Bogar, F., Megyeri, K., Ling, I., Barkoczy, J., et al. (2017). Loop-F of the alpha-subunit determines the pharmacologic profile of novel competitive inhibitors of GABA_A receptors. *Eur. J. Pharmacol.* 798, 129–136. doi: 10.1016/j.ejphar.2017.01.033
- Moraga-Cid, G., Sauguet, L., Huon, C., Malherbe, L., Girard-Blanc, C., Petres, S., et al. (2015). Allosteric and hyperekplexic mutant phenotypes investigated on an alpha1 glycine receptor transmembrane structure. *Proc. Natl. Acad. Sci. U.S.A.* 112, 2865–2870. doi: 10.1073/pnas.1417864112
- Morales-Perez, C. L., Novello, C. M., and Hibbs, R. E. (2016). X-ray structure of the human alpha4beta2 nicotinic receptor. *Nature* 538, 411–415. doi: 10.1038/nature19785
- Nys, M., Kesters, D., and Ulens, C. (2013). Structural insights into Cys-loop receptor function and ligand recognition. *Biochem. Pharmacol.* 86, 1042–1053. doi: 10.1016/j.bcp.2013.07.001
- Nys, M., Wijckmans, E., Farinha, A., Yoluk, O., Andersson, M., Brams, M., et al. (2016). Allosteric binding site in a Cys-loop receptor ligand-binding domain unveiled in the crystal structure of ELIC in complex with chlorpromazine. *Proc. Natl. Acad. Sci. U.S.A.* 113, E6696–E6703. doi: 10.1073/pnas.1603101113
- Padgett, C. L., and Lummis, S. C. (2008). The F-loop of the GABA A receptor gamma2 subunit contributes to benzodiazepine modulation. *J. Biol. Chem.* 283, 2702–2708. doi: 10.1074/jbc.M705699200
- Pilorge, M., Fassier, C., Le Corronc, H., Potey, A., Bai, J., De Gois, S., et al. (2015). Genetic and functional analyses demonstrate a role for abnormal glycinergic signaling in autism. *Mol. Psychiatry* 21, 936–945. doi: 10.1038/mp.2015.139
- Pless, S. A., Hanek, A. P., Price, K. L., Lynch, J. W., Lester, H. A., Dougherty, D. A., et al. (2011). A cation-pi interaction at a phenylalanine residue in the glycine receptor binding site is conserved for different agonists. *Mol. Pharmacol.* 79, 742–748. doi: 10.1124/mol.110.069583
- Rajendra, S., Lynch, J. W., and Schofield, P. R. (1997). The glycine receptor. *Pharmacol. Ther.* 73, 121–146. doi: 10.1016/S0163-7258(96)00163-5
- Schaefer, N., Berger, A., van Brederode, J., Zheng, F., Zhang, Y., Leacock, S., et al. (2017). Disruption of a structurally important extracellular element in the glycine receptor leads to decreased synaptic integration and signaling resulting in severe startle disease. *J. Neurosci.* 37, 7948–7961. doi: 10.1523/JNEUROSCI.0009-17.2017
- Schaefer, N., Kluck, C. J., Price, K. L., Meiselbach, H., Vornberger, N., Schwarzing, S., et al. (2015). Disturbed neuronal ER-golgi sorting of unassembled glycine receptors suggests altered subcellular processing is a cause of human hyperekplexia. *J. Neurosci.* 35, 422–437. doi: 10.1523/JNEUROSCI.1509-14.2015
- Schindelin, J., Arganda-Carreras, I., Frise, E., Kaynig, V., Longair, M., Pietzsch, T., et al. (2012). Fiji: an open-source platform for biological-image analysis. *Nat. Methods* 9, 676–682. doi: 10.1038/nmeth.2019
- Schindelin, J., Rueden, C. T., Hiner, M. C., and Eliceiri, K. W. (2015). The ImageJ ecosystem: an open platform for biomedical image analysis. *Mol. Reprod. Dev.* 82, 518–529. doi: 10.1002/mrd.22489
- Schneider, C. A., Rasband, W. S., and Eliceiri, K. W. (2012). NIH Image to ImageJ: 25 years of image analysis. *Nat. Methods* 9, 671–675. doi: 10.1038/nmeth.2089
- Sievers, F., Wilm, A., Dineen, D., Gibson, T. J., Karplus, K., Li, W., et al. (2011). Fast, scalable generation of high-quality protein multiple sequence alignments using Clustal Omega. *Mol. Syst. Biol.* 7, 539. doi: 10.1038/msb.2011.75
- Villmann, C., Oertel, J., Melzer, N., and Becker, C. M. (2009). Recessive hyperekplexia mutations of the glycine receptor alpha1 subunit affect cell surface integration and stability. *J. Neurochem.* 111, 837–847. doi: 10.1111/j.1471-4159.2009.06372.x
- Vogel, N., Kluck, C. J., Melzer, N., Schwarzing, S., Breiting, U., Seeber, S., et al. (2009). Mapping of disulfide bonds within the amino-terminal extracellular domain of the inhibitory glycine receptor. *J. Biol. Chem.* 284, 36128–36136. doi: 10.1074/jbc.M109.043448
- Yang, Z., Taran, E., Webb, T. I., and Lynch, J. W. (2012). Stoichiometry and subunit arrangement of alpha1beta glycine receptors as determined by atomic force microscopy. *Biochemistry* 51, 5229–5231. doi: 10.1021/bi300063m
- Yu, R., Hurdiss, E., Greiner, T., Lape, R., Sivilotti, L., and Biggin, P. C. (2014). Agonist and antagonist binding in human glycine receptors. *Biochemistry* 53, 6041–6051. doi: 10.1021/bi500815f
- Zhou, N., Wang, C. H., Zhang, S., and Wu, D. C. (2013). The GLRA1 missense mutation W170S associates lack of Zn²⁺ potentiation with human hyperekplexia. *J. Neurosci.* 33, 17675–17681. doi: 10.1523/JNEUROSCI.3240-13.2013

Conflict of Interest Statement: The authors declare that the research was conducted in the absence of any commercial or financial relationships that could be construed as a potential conflict of interest.

Copyright © 2017 Janzen, Schaefer, Delto, Schindelin and Villmann. This is an open-access article distributed under the terms of the Creative Commons Attribution License (CC BY). The use, distribution or reproduction in other forums is permitted, provided the original author(s) or licensor are credited and that the original publication in this journal is cited, in accordance with accepted academic practice. No use, distribution or reproduction is permitted which does not comply with these terms.